Sedwick, W. D., Wang, T. S.-F., & Korn, D. (1975) *J. Biol. Chem. 250*, 7045–7056.
Spanos, A., Sedwick, S. G., Yarranton, S. T., Hubscher, U., & Banks, G. R. (1981) *Nucleic Acids Res. 9*, 1825–1839.
Tanaka, S., Hu, S., Wang, T. S.-F., & Korn, D. (1982) *J. Biol. Chem. 257*, 8386–8390.
Towbin, H., Staehelin, T., & Gordon, J. (1979) *Proc. Natl. Acad. Sci. U.S.A. 76*, 4350–4354.
Wahl, A. F., Kowalski, S. P., Harwell, L. W., Lord, E. M., & Bambara, R. A. (1984) *Biochemistry 23*, 1895–1899.
Wang, T. S.-F., Hu, S. Z., & Korn, D. (1984) *J. Biol. Chem. 259*, 1854–1865.
Waqar, M. A., Evans, M. J., & Huberman, J. A. (1978) *Nucleic Acids Res. 6*, 1933–1946.

DNA Binding Specificity of a Series of Cationic Metalloporphyrin Complexes†

Brian Ward, Andrew Skorobogaty, and James C. Dabrowiak*
Department of Chemistry, Syracuse University, Syracuse, New York 13244-1200
Received March 12, 1986; Revised Manuscript Received July 7, 1986

ABSTRACT: The sequence specificities of a series of cationic metalloporphyrins toward a 139 base pair restriction fragment of pBR-322 DNA have been studied by DNase I footprinting methodology. Analysis using controlled digests and quantitative autoradiography/microdensitometry revealed that the 5- and 6-coordinate complexes of *meso*-tetrakis(*N*-methyl-4-pyridiniumyl)porphine, MT4MPyP, where M is Mn, Fe, Co, and Zn, were found to bind to AT regions of DNA. Footprinting analysis involving the radiolabel on the opposing strand of restriction fragment showed site skewing in the direction of the 3′ end of the fragment, indicating that the porphyrins bind in the minor groove of DNA. The significant increase in DNase I catalyzed hydrolysis observed in various regions of the fragment appeared to be primarily due to a decrease in available substrate DNA upon porphyrin binding with possible contributions from structural changes in DNA caused by ligand binding. The complexes NiT4MPyP and CuT4MPyP were found to bind to both AT and GC regions of the fragment, producing different degrees of inhibition in the two regions. Since the outside-binding porphyrins can neither intercalate or effectively hydrogen bond to DNA, they appear to read sequence by responding to steric and/or electrostatic potential effects located in the minor groove of DNA.

The interaction of metalloporphyrins with DNA has been the subject of a number of investigations. The basis for these studies is in part related to the observation that certain porphyrins can serve as photo sensitizers for destruction of tumor cells. This effect, termed photodynamic therapy, has been useful for treatment of a number of tumors that occur in man (Kelly et al., 1975; Dougherty et al., 1979). In addition to the photodynamic properties of the porphyrins, the Fe^{3+} complex of protoporphyrin IX, hemin, is believed to play an important role in the differentation of Friend erythroleukemia cells (Lo et al., 1981). Since porphyrin-mediated DNA damage may take place during this process (Scher & Friend, 1978), efforts have been made to detect porphyrin-induced DNA strand scission in vitro. In this regard it has been shown that hemin in the presence of 2-mercaptoethanol and oxygen can efficiently degrade the closed circular plasmid pBR-322 (Aft & Mueller, 1983).

Metalloporphyrins have also been reported to possess antitumor properties (Lown et al., 1984). Covalent attachment of the DNA binding groups acridine or acodazole to hemin results in bleomycin-like porphyrin compounds, which in addition to exhibiting in vivo antitumor effects are capable of binding to and degrading PM2-DNA (Lown & Joshua, 1982). Studies of the degradation process with natural DNAs of definded sequence have shown that these compounds cleave DNA in a sequence neutral manner (Lown et al., 1986). Nuclease activity has also been observed for ferric porphyrins possessing the appended potent mutagen 2-amino-6-methyldipurido[1,2-*a*:3′2′-*d*]imidazole (Hashimota et al., 1984). However, in this case studies with a restriction fragment from pBR-322 DNA revealed that porphyrin-induced DNA cleavage is sequence specific and is similar to that of the anticancer agent bleomycin (Dabrowiak, 1983).

The most actively studied DNA binding metalloporphyrins are the metal complexes of the tetracationic water-soluble compound *meso*-tetrakis(*N*-methyl-4-pyridiniumyl)porphine, H_2T4MPyP[1] (Fiel et al., 1985; Pasternack et al., 1984; Kelly et al., 1985; Marzilli et al., 1986). Kinetic (Pasternack et

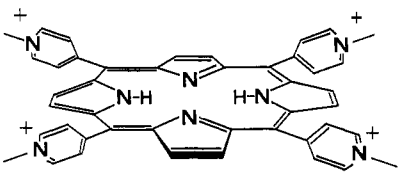

al., 1983a,b), optical (Carvlin & Fiel, 1983), and other physiochemical evidence (Dougherty et al., 1985) suggests that the nature of the coordinated metal ion controls the porphyrin-binding mechanism and its DNA base preference. At low

† This work was supported by grants from the National Institutes of Health (GM31895) and the Bristol Myers Co.

[1] Abbreviations: T4MPyP, dianion of *meso*-tetrakis(*N*-methyl-4-pyridiniumyl)porphine; MPE, methidium–propyl–iron ethylenediaminetetraacetic acid; DNase, deoxyribonuclease; TPP, *meso*-tetraphenylporphine; Tris-HCl, tris(hydroxymethyl)aminomethane hydrochloride; EDTA, ethylenediaminetetraacetic acid.

0006-2960/86/0425-7827$01.50/0

values of polymer loading, the Cu^{2+} and Ni^{2+} complexes of $H_2T4MPyP$ bind by intercalation to GC-rich regions of DNA while the analogous Mn^{3+}, Fe^{3+}, Co^{3+}, and Zn^{2+} compounds bind through a nonintercalative process to AT regions of the polymer. Circular dichroism studies show that the metal-free ligand $H_2T4MPyP$ can bind to both GC- and AT-rich regions of DNA (Pasternack et al., 1983b). In addition to modulating base preference and binding mode through changes in the nature of the coordinated metal ion, it is also possible to alter DNA binding specificity by structurally modifying the porphyrin framework (Carvlin & Fiel, 1983; Carvlin et al., 1982). For example, DNA binding studies with *meso*-tetrakis(*N*-methyl-2-pyridiniumyl)porphine showed that substituents on the porphyrin ring that extend above and below the porphyrin plane can block the intercalative binding mode of the metalloporphyrin. Aside from simply binding to DNA, certain of the cationic porphyrins can be chemically or photochemically activated to induce DNA strand scission (Fiel et al., 1982; Kelly et al., 1985).

In this paper we present the binding sequence specificity of MT4MPyP, where M is Mn^{3+}, Fe^{3+}, Co^{3+}, Ni^{2+}, Cu^{2+}, and Zn^{2+}, toward a 139 base pair restriction fragment of pBR-322 DNA using DNase I footprinting methodology (Galas & Schmitz, 1978; Lane et al., 1983). Analysis involving quantitative autoradiography/microdensitometry (Dabrowiak et al., 1986) revealed that the outside-binding metalloporphyrins, Mn^{3+}, Fe^{3+}, Co^{3+}, and Zn^{2+}, exhibit a high degree of AT binding specificity. Studies involving the labeled opposing strand of the restriction fragment revealed that a binding site for MnT4MPyP is skewed in the direction of the 3′ end of the polymer, indicating that compound binding takes place in the minor groove of DNA. The observation that CuT4MPyP and NiT4MPyP inhibit the enzyme in both AT and GC regions was interpreted in terms of different types of porphyrin binding taking place in those regions, i.e., intercalation (GC) and outside binding (AT). Footprinting studies with the unmetalated porphyrin $H_2T4MPyP$, employing the conditions used for the metal complexes, did not result in site-specific DNase I inhibition. Porphyrin perturbation of the enzyme–DNA equilibrium and possible DNA structural changes induced by porphyrin binding are suggested as being responsible for the observed increases in cleavage rate at various sites on the restriction fragment.

Materials and Methods

The metalloporphyrins used in the study were prepared by the method of Pasternack et al. (1983b) and their concentrations in aqueous solution determined with published extinction coefficients. The concentration of sonicated calf thymus DNA, in base pairs, was determined optically with ϵ_{260} of 13 100 cm^{-1} M^{-1}.

The *Hin*dIII–*Nci*I restriction fragment of pBR-322 DNA was 3′ end labeled by filling in an A at position 33 or a G at position 172 of the fragment with [α-^{32}P]dXTP and reverse transcriptase (Lown et al., 1986). The numbering index of the fragment is the same as the genomic numbering system for pBR-322 DNA (Maniatis et al., 1982). Checks on the integrity of the fragment with denaturing polyacrylamide gel electrophoresis revealed that the fragment had not sustained cleavage during the labeling and isolation procedures.

Unless otherwise stated, all solutions for footprinting experiments were in 50 mM Tris-HCl, pH 7.0 buffer. Thus, solutions for footprinting experiments were prepared by mixing 2 μL of sonicated calf thymus DNA (770 μM base pairs), 2 μL of fragment ($\sim$7 μM), 2 μL of buffer or porphyrin solution of the complex, and 2 μL of activated enzyme complex (Lown et al., 1986). Prior to addition of enzyme and digestion for 10 min at 37 °C, the DNA–porphyrin mixtures were preincubated for 90 min at 37 °C. The digests were terminated by the addition of 10 μL of a solution containing 70% aqueous urea, 20 mM EDTA, and 0.025% each of bromophenol blue and xylene cyanol and followed by heating to 80 °C for 10 min. For each porphyrin, DNase I digests were carried out for 10–12 ratios of porphyrin to DNA base pairs (r_t). The values of r_t studied were in the range $0.001 \leq r_t \leq 0.5$.

Unless otherwise noted, all digests were terminated so as to leave $\sim$70 $\pm$ 5% of the full-length fragment uncleaved (Goodisman & Dabrowiak, 1985). The reaction conditions were established by digesting the fragment in the absence of porphyrin with DNase I, separating the products via polyacrylamide gel electrophoresis, excising the full-length fragment from the gel, and subjecting it to scintillation counting.

Electrophoresis of the oligonucleotide products was performed on an in-house-developed thermostated field gradient electrophoresis device. After the DNA solutions were loaded onto a 12% denaturing polyacrylamide gel, electrophoresis was carried out at $\sim$50 °C for $\sim$2 h with an applied power of 150–175 W in a 90 mM Tris–borate and 2 mM EDTA, pH 8.3, buffer. Autoradiography was accomplished with unpreflashed Kodak XAR-5 X-ray film. Autoradiographic exposure times were such that the maximum optical density of any of the analyzed bands was in the linear response range of the photographic emulsion, OD <1. With the previously described computer–microdensitometer system (Dabrowiak et al., 1986), the bands were scanned linearly, in the direction of electrophoresis, through their short dimensions. For the purpose of analysis, a 70–90% reduction in the concentration of a particular oligomer at r_t of 0.25 was referred to as a strong inhibition, while a weak inhibition constituted a 50–70% reduction in oligomer concentration at the same value of r_t. Since reduction in the enzymatic cleavage rate has not yet been correlated with a ligand binding constant, no accessment of the latter from the data presented could be made. Nucleotide positions where the cleavage rate of the enzyme in the presence of the porphyrin was above the control are referred to as enhancements. Establishment of sequence involved guanine-specific cleavage of DNA (Maxam & Gilbert, 1980) and reference to the cleavage pattern of the fragment in the presence of DNase I (Lown et al., 1986).

Porphyrin precipitation of DNA was checked at an r_t of 0.5. Thus, 10 μL of sonicated calf thymus DNA (770 μM in base pairs) was added to 30 μL of an appropriate concentration of the metalloporphyrin in 50 mM Tris-HCl, pH 7.0 buffer and allowed to equilibrate as for the footprinting experiments. The samples were centrifuged in a microcentrifuge and inspected for the presence of a colored pellet.

Results

An autoradiogram of a footprinting experiment with the cationic metalloporphyrins, CoT4MPyP and FeT4MPyP, and the *Hin*dIII/*Nci*I 139 base pair restriction fragment of pBR-322 DNA is shown in Figure 1. Densitometric scans of selected lanes of Figure 1 as well as of lanes of other footprinting autoradiograms involving the metalloporphyrins M(T4MPyP), where M is Mn^{3+}, Zn^{2+}, Ni^{2+}, and Cu^{2+}, are shown in Figures 2–8. The inhibition and enhancement information obtained in the study is summarized on the sequence of the restriction fragment shown in Figure 9.

Figures 2–5 show that the Mn, Fe, Co, and Zn porphyrins affect enzymatic cleavage of the fragment similarly. Of the $\sim$60 analyzed cutting sites on the fragment, enzymatic inhibitions were observed at positions 83–97 and 54–68, which

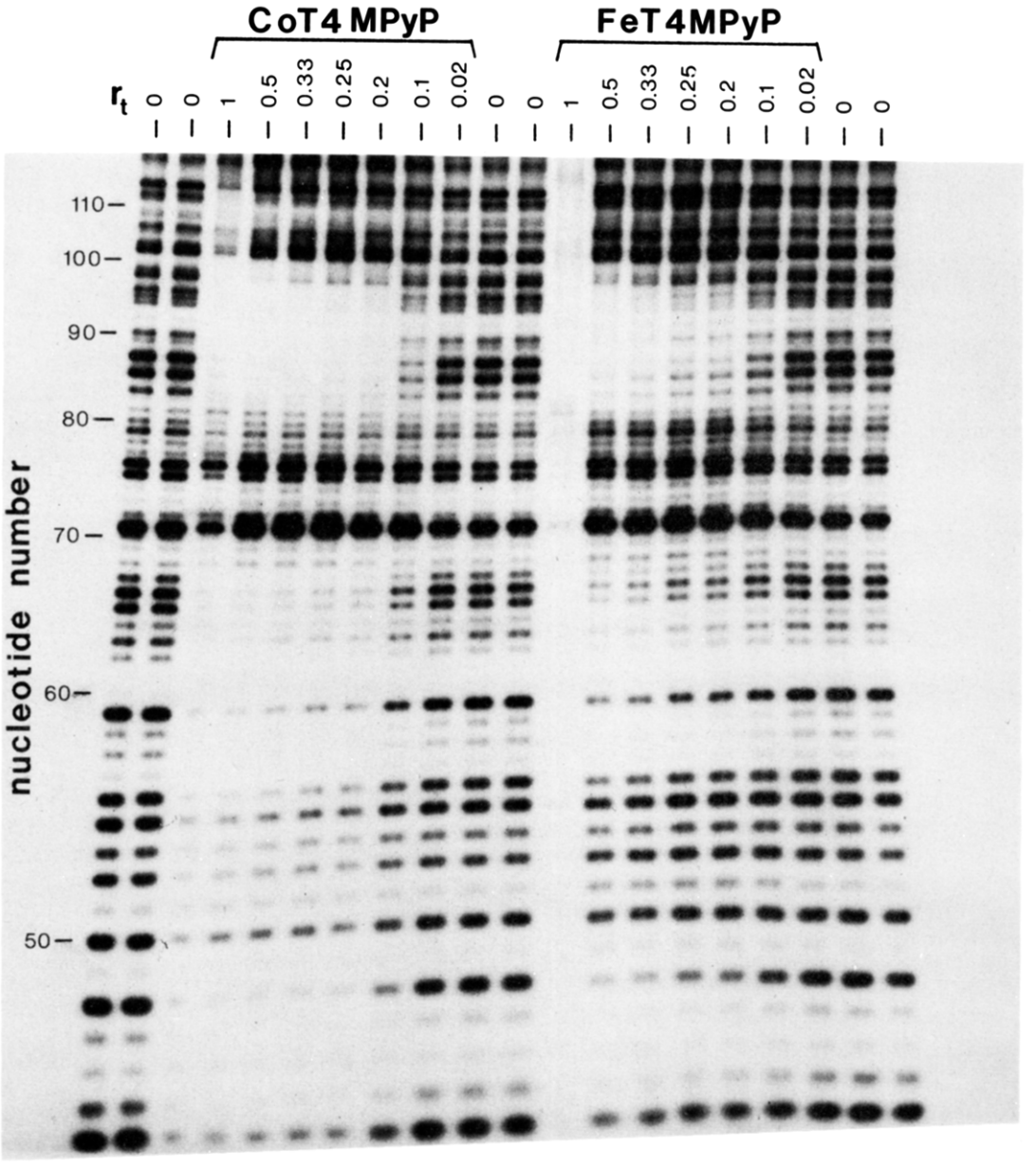

FIGURE 1: An autoradiogram of a DNase I footprinting experiment with CoT4MPyP and FeT4MPyP at various values of the compound-to-DNA base pair ratio (r_t) is shown. The values of r_t are indicated above the respective lanes. The numbering system used is the genomic numbering system of pBR-322 DNA (Maniatis et al., 1982).

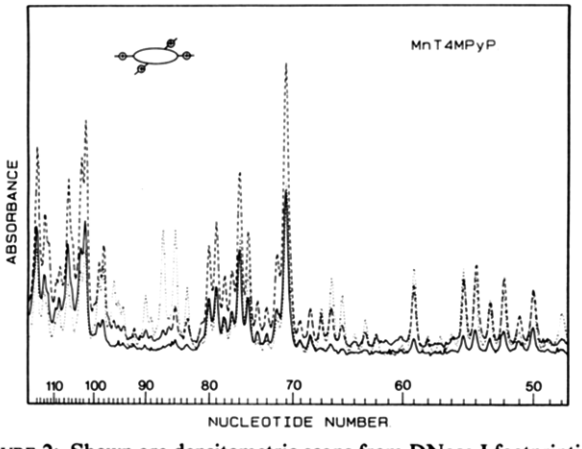

FIGURE 2: Shown are densitometric scans from DNase I footprinting experiments (label at position 33) involving MnT4MPyP: DNase I (···); r_t 0.25 (--); r_t, 0.5 (—).

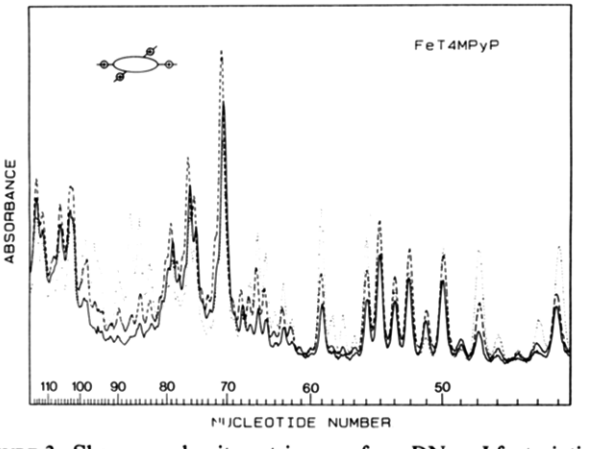

FIGURE 3: Shown are densitometric scans from DNase I footprinting experiments (label at position 33) involving FeT4MPyP: DNase I (···); r_t, 0.25 (--); r_t, 0.50 (—).

have sequences of 3′-ACATACTTTAGATTG-5′ and 3′-TCAATTTAACGATTG-5′, respectively. Both regions are 15 nucleotides long and contain a percentage of A·T base pairs (73%), which is above the A·T composition of the analyzed

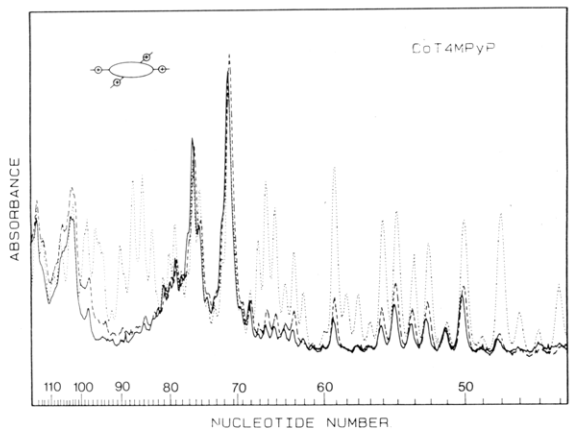

FIGURE 4: Shown are densitometric scans from DNase I footprinting experiments (label at position 33) involving CoT4MPyP: DNase I (···); r_t, 0.25 (−−); r_t, 0.50 (—).

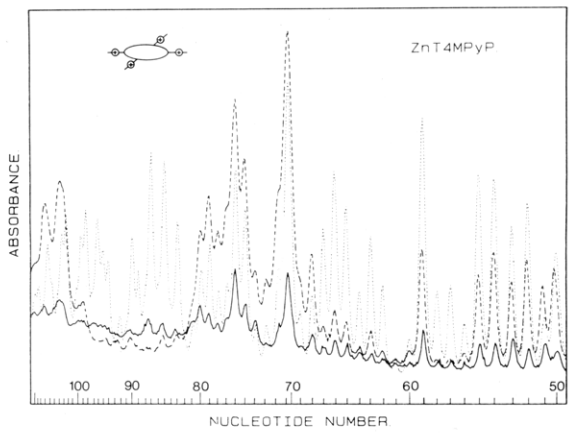

FIGURE 5: Shown are densitometric scans from DNase I footprinting experiments (label at position 33) involving ZnT4MPyP: DNase I (···); r_t, 0.25 (−−); r_t, 0.50 (—).

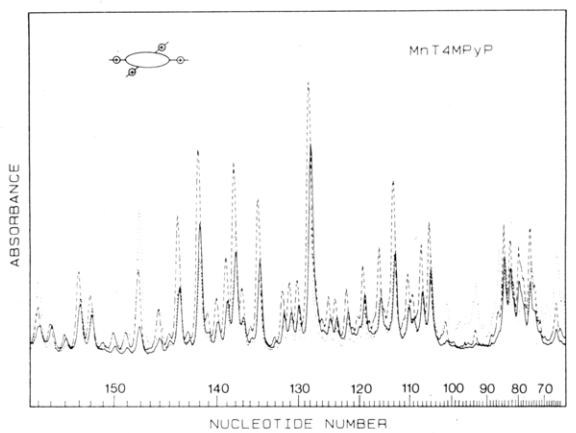

FIGURE 6: Shown are densitometric scans from DNase I footprinting experiments (label at position 172) involving MnT4MPyP: DNase I (···); r_t, 0.25 (−−); r_t, 0.50 (—).

portion of the fragment (62%). For Mn, Fe, and CoT4MPyP an additional inhibition region at positions 42–48 having the sequence 3′-CATCAA-5′ could also be observed. The Zn analogue very likely possesses the latter region as well, but due to an increase in the time of electrophoresis for this complex, the oligomers "scoring" the site did not appear on the autoradiogram. Inspection of the densitometric data for r_t of 0.25, Figures 2–5, revealed that the effects of porphyrin-induced enzymatic inhibition is greatest for CoT4MPyP. Interestingly, the binding of MnT4MPyP, FeT4MPyP, or ZnT4MPyP to the fragment caused an *increase* in the enzymatic cleavage

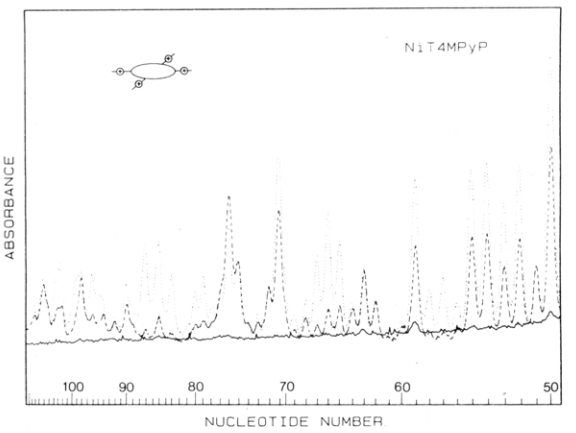

FIGURE 7: Shown are densitometric scans from DNase I footprinting experiments involving NiT4MPyP: DNase I (···); r_t, 0.25 (−−); r_t, 0.50 (—). The amont of full-length undigested DNA remaining at digest termination was ~50% of its original value.

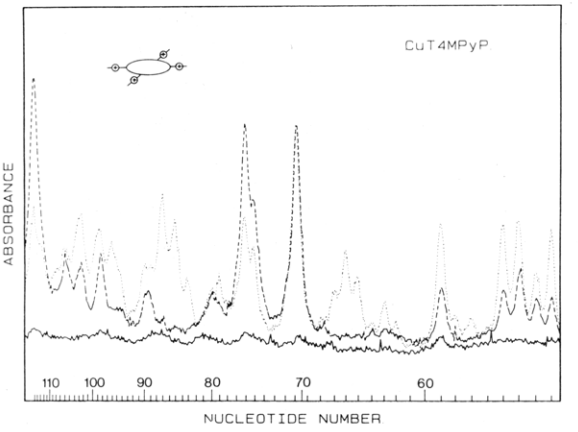

FIGURE 8: Shown are densitometric scans from footprinting experiments involving CuT4MPyP: DNase I (···); r_t, 0.25 (−−); r_t, 0.50 (—).

rate at positions 68–80 having the sequence 3′-GTCAGTCCGTG-5′. For the cobalt complex, no significant rate enhancements among the ~60 analyzed cleavage sites were noted (Figure 4). At r_t of 0.5, the highest value of r_t studied, these metalloporphyrins were unable to totally inhibit DNase I cleavage of the fragment (Figures 2–5).

Densitometric scans of a footprinting autoradiogram experiment involving the fragment labeled at position 172 (G) and MnT4MPyP are shown in Figure 6. The opposite strand data revealed a large, strong, AT-rich inhibition at positions 85–101 having the sequence 5′-TATGAAATCTAACAATG-3′ as well as a smaller protection at 146–148, 5′-ATA-3′. As is evident from Figures 2, 6, and 9, the opposing strand protections do not overlap on the sequence of the fragment but rather are advanced in the 3′ direction of the molecule. Figures 6 and 9 also show that enhancements are observed at every DNase I cleavage site in the GC-rich regions, 104–145 and 150–155, of the fragment.

As shown in Figures 7 and 8, NiT4MPyP and CuT4MPyP induced changes in the enzymatic cleavage rate, which, although similar to each other, were significantly different than that of the aforementioned group of metalloporphyrins. Inspection of the autoradiographic data revealed that for both compounds changes in the enzyme cleavage pattern in the range $0 < r_t < \sim 0.2$ were not detectable. At r_t values of $> \sim 0.2$, binding of NiT4MPyP to the fragment was observed to give rise to strong inhibitions at positions 56–60, 65–67, 79–90, and 94–97, while weaker inhibitions were found at

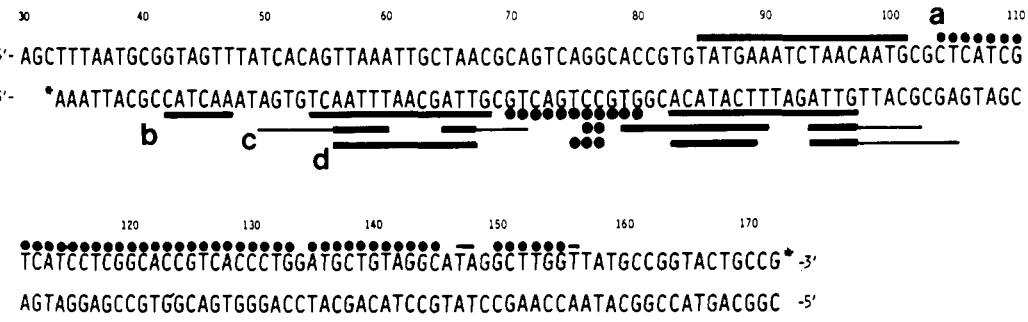

FIGURE 9: The sequence of the 139 base pair restriction fragment from pBR-322 DNA is shown. The regions of strong (—) and weak (—) inhibition as well as enhancements (●) are indicated. Experiments involving the fragment labeled at position 33 (A) were as follows: (b) Mn, Fe, Co, and ZnT4MPyP; (c) NiT4MPyP; (d) CuT4MPyP. The inhibition patterns of MnT4MPyP (a) were also examined with the fragment labeled at position 172 (G). The numbering system used is the genomic numbering system of pBR-322 DNA (Maniatis et al., 1982).

positions 50–55, 68–72, and 98–102 (Figure 9). Although the inhibitions varied in length, 4–12 nucleotides, the strong inhibitions possessed a high percentage of A·T base pairs while for the weaker sites G·C base pairs predominated. This compound exhibited intensity enhancements at positions 76 and 77, 3′-CC-5′ of the fragment (Figure 7).

The copper compound exhibited strong protections at positions 56–67, 83–89, and 93–97, each containing a high percentage of A·T base pairs, while the weak site at 98–105 was found to contain only 50% A·T base pairs. For this complex, intensity enhancements were observed at positions 75–77 having the sequence 3′-TCC-5′. In this case, as with NiT4MPyP, DNase I cleavage of the fragment was totally inhibited at r_t of 0.5 (Figures 7 and 8).

At an r_t of 0.5, one metalloporphyrin from each group was examined for its ability to precipitate DNA. When MnT4MPyP and NiT4MPyP were each incubated with sonicated claf thymus DNA, colored pellets were observed after centrifugation. No precipitates were observed for the porphyrin or DNA solutions alone.

Autoradiograms of footprinting experiments involving the free base H_2T4MPyP (data not shown) revealed that in the range $0 < r_t \leq 0.25$ the cleavage pattern of the enzyme was unaffected by added porphyrin. At r_t values in the range $0.25 < r_t \leq 0.5$, DNase I cleavage of the fragment uniformly decreased at all sites. No DNA cleavage occurred at the highest value of r_t studied (0.5), indicating that DNA precipitation had occurred.

Discussion

The metalloporphyrin compounds used in this study are rigid structures possessing four positive charges located on the alkylated pyridine residues of the macrocycle. Although X-ray crystallographic analyses of these compounds have not been reported, their structural features are expected to be similar to those of the well-studied complexes of *meso*-tetraphenylporphine, TPP (Hoard, 1971). Thus, due to steric interactions the plane of the pyridinium rings of T4MPyP, like the phenyl rings of TPP, is expected to be out-of-plane with respect to the porphyrin plane. At neutral pH, the Mn^{3+}, Fe^{3+}, Co^{3+}, and Zn^{2+} complexes are 5- and 6-coordinate, having axial ligands (e.g., OH^- and H_2O) displaced above and below the porphyrin plane. Although compounds of TPP are known to form μ-oxo-bridged dimers in solution, e.g., $[Fe(TPP)]_2O$, and under certain conditions to self-associate, neither appears to be of great importance for the cationic metalloporphyrins in aqueous media (Pasternack et al., 1977). In aqueous solution the 4-coordinate complex, NiT4MPyP, is known to be in equilibrium with a 6-coordinate diaquo species, NiT4MPyP-$(H_2O)_2$ (Pasternack et al., 1973). However, optical studies indicate that in the presence of DNA this equilibrium is shifted in favor of the 4-coordinate structure. The d^9 metal complex, CuT4MPyP, shows little tendency to bind axial ligands and thus is exclusively 4-coordinate in aqueous solution.

Consideration of the structure of the cationic porphyrins and DNA permits some insight into the structural features associated with the binding mechanism. Molecular models show that the porphyrin ligand is ~20 Å in its longest dimension, and thus the compounds are capable of spanning five to six base pairs in B-form DNA (Saenger, 1982). As has been shown by a number of physiochemical studies (Pasternack et al., 1983a,b; Carvlin & Fiel, 1983), the 4-coordinate complexes NiT4MPyP and CuT4MPyP can intercalate in between the base pairs of DNA in GC-rich regions of the polymer. Models also show that, due to the severe steric demands of the axially bonded groups, the complexes MnT4MPyP, FeT4MPyP, CoT4MPyP cannot bind to DNA via intercalation and therefore must utilize an outside binding mechanism exclusively. For both 4-coordinate or 5- and 6-coordinate tetracationic porphyrins, models show it is possible to have "end-on" binding in either the major or minor groove of B-DNA such that the metalloporphyrin z axis (C_4 symmetry axis) is tangential to the helical surface of the polymer. The important factors in this case are the van der Waals width of the alkylated pyridine rings, their orientations relative to the porphyrin plane, and the widths of the two grooves of DNA.

Also noteworthy in connection with the metalloporphyrin DNA interaction is the fact that the porphyrin framework itself is devoid of any H-bonding donor/acceptor capacity. Although H bonding between DNA and groups occupying the axial sites of the compounds is a possibility, the porphyrin DNA binding mechanism should be largely electrostatic in nature.

Mn, Fe, Co, and Zn Complexes of T4MPyP. As can be seen in Figure 9, the metalloporphyrin compounds MnT4MPyP, FeT4MPyP, CoT4MPyP, and ZnT4MPyP bind to AT-rich regions of the restriction fragment. Consideration of opposite-strand data in the case of MnT4MPyP showed that the long protection centered at position 91 of the fragment is skewed in the 3′ direction of the molecule. Since, similar skewing has been observed for the anticancer agent actinomycin D (Lane et al., 1985) in footprinting experiments and for a variety of poly(*N*-methylpyrrole) DNA-cleaving agents [Schultz and Dervan (1984) and references cited therein], the 5- and 6-coordinate porphyrins, like the former ligands, most probably bind in the minor groove of DNA.

The length of the DNase I inhibitions in the regions 54–68 and 83–97 and the size of the metalloporphyrins suggest that three to four separate porphyrin binding sites may be located within the two 15 base pair inhibition regions of the fragment. Although the minimum porphyrin binding site is difficult to ascertain from the data available, the three-nucleotide sequence 5′-ATA-3′, 146–148, is capable of binding the metallo-

porphyrins (Figures 6 and 9).

Two possible sources for the observed increase in enzymatic cleavage at positions 68–80, 104–145, and 150–155 of the fragment can be advanced. (Figures 2–6 and 9). As has been shown by Brenowitz et al. (1986) in DNase I footprinting studies involving protein–DNA interactions, the increased cleavage rate observed between the inhibition regions may be due to a reduction of the available DNA as substrate due to blockage by the ligand. This effect may be more pronounced for small ligands such as the metalloporphyrins, since when compared to proteins the latter exhibit lower sequence specificity and are thus able to block a larger amount of DNA from cleavage by the enzyme. For controlled digests having constant enzyme and DNA concentrations, *increasing* the ligand concentration has the affect of *increasing* the enzymatic cleavage rate in regions of the polymer where no binding is taking place. As is evident from Figures 1–6, this effect may be operative for values of r_t in the range $0 \leq r_t \leq 0.25$, but as the highest value of r_t is reached, r_t of 0.5, the concentrations of all oligomers are below those of their DNase I controls. From Figures 7 and 8 this effect occurs for Cu and NiT4MPyP at r_t values above 0.25 but less than 0.5. The latter phenomenon appears to be related to the observation that at high values of r_t the porphyrins precipitate DNA from solution. Upon removal from solution, the DNA cannot be attacked by DNase I, and thus the total amount of oligomers produced in the digest is reduced.

A second possible contribution for the observed rate increases may be due to ligand-induced structural changes in DNA. For example, the porphyrin may alter base pair twist angles near the sites of binding. Since changes in the twist angle are known to lead modified rates of DNase I catalyzed phosphodiester hydrolysis (Dickerson & Drew, 1981; Drew, 1984; Drew & Travers, 1984), enhancements may in part be structural in origin. However, consideration of the locations of the enhancements especially in the region 104–145, Figure 9, relative to the nearest porphyrin-binding sites, ~100 and ~147, strongly suggests that at least in this region of the fragment the predominant effect giving rise to the rate enhancements is caused by an increase in the available enzyme to free DNA ratio as binding sites load with porphyrin.

The fact that Fe-, Mn-, Co-, and ZnT4MPyP displayed very similar inhibition patterns, Figures 2–5 and 9, yet footprinting involving CoT4MPyP uncovered no rate enhancements suggests that the hypersensitivity mechanism may also be sensitive to the identity of the central metal ion. One may contend that CoT4MPyP binding also caused DNase I cleavage rate enhancements but it was not observed due to precipitation, which fortuitously equaled the amount of enhancement. This however is not expected to be the case since the tendency to precipitate DNA, Figures 1–8, appears to be least for CoT4MPyP. These observations suggest that DNase I hypersensitivity due to ligand binding may, at least in part, be due to porphyrin-induced structural perturbations in the polymer.

Although comparative footprinting studies with the anticancer agent actinomycin D and the probes DNase I and the synthetic DNA-cleaving agent MPE (Van Dyke & Dervan, 1983) have revealed that both the enzyme and MPE report similar binding information, the possibility that DNase I is inhibited in regions of the polymer not actually occupied by a ligand exists. This issue may be clarified by the development of other nuclease active probes that recognize DNA in a manner dissimilar to DNase I. Development of such probes and an assessment of kinetic vs. structural effects between drug binding to DNA and DNase I cleavage rates are points of active research in our laboratory.

Porphyrin Binding to DNA. Interestingly, the 5- and 6-coordinate metalloporphyrins utilize the same binding sequences on the restriction fragment as the antiviral agent netropsin (Lane et al., 1983). The reason for the similarity in binding is unclear, but in light of the structures of the metalloporphyrins, specific H-bonding contacts, as occur between netropsin and DNA (Kopka et al., 1985a,b), cannot be part of the porphyrin-binding mechanism. It may be that the actual reading of the sequence by the porphyrin is accomplished through electrostatic/van der Waals interactions between the macrocycle and DNA (Weiner et al., 1982; Pullman, 1983).

Recent theoretical calculations for $(dA)_{11}\cdot(dT)_{11}$ vs. $(dG)_{11}\cdot(dC)_{11}$ have predicted that the surface potential minima in the grooves of these molecules are highly dependent upon environmental effects (Lavery & Pullman, 1985). For *unscreened* phosphate oxygens in vacuo, the predicted order of increasing potentials was AT minor < GC major < GC minor < AT major. Similar calculations for *screened* phosphates in vacuo and in water yielded orders of AT minor ~ GC major < GC minor < AT major and GC major < AT minor < GC minor < AT major, respectively. Considering the above environmental effects, one would predict that the binding of a molecule in a groove of DNA via an electrostatic attraction would favor the AT minor groove over the GC major groove in vacuo with unscreened phosphates by approximately 10^5 (i.e., AT minor was more negative than GC major by 7 kcal/mol). Similarly, screening in vacuo provides no preference while in water with the phosphates screened the GC major groove would be favored over the AT minor groove by ~150 (GC major groove more negative by 3 kcal/mol). The results obtained here show that the 5- and 6-coordinate complexes bind in the minor groove of AT-rich regions of natural DNA, a result most consistent with the unscreened in vacuo calculations.

The 2-amino group of guanine, which is located in the minor groove of DNA, may also be a factor discouraging porphyrin binding to sequences containing G·C base pairs. This group projects above the floor of the minor groove and in the absence of hydrogen-bond acceptor sites on the porphyrin may serve to prevent ligand binding through steric effects (Kopka et al., 1985a,b).

Cu and Ni Complexes of T4MPyP. From Figure 9 it is apparent that binding Cu- or NiT4MPyP to DNA results in two different extents of DNase I cleavage rate inhibition. The first, termed strong, overlaps significantly with the binding sites for the 5- and 6-coordinate porphyrins, while the sites termed weak are in regions with diminished AT populations relative to the strong sites. The most reasonable explanation for the presence of the strong and weak inhibitions for these two compounds is that they exhibit two different binding modes toward DNA, both of which are seen by DNase I. If two different modes of binding are taking place, there seems to be no necessity to invoke that each mode will perturb DNA in such a way so as to cause an equal decrease in the extent of digestion. Since other workers have provided physiochemical evidence that Cu- and NiT4MPyP can bind to DNA via an intercalative process (Pasternack et al., 1983a,b; Carvlin & Fiel, 1983; Dougherty et al., 1985) and that this mode of binding should be favored in GC-rich regions of the polymer, it is felt that the weaker inhibitions for Cu- and NiTMPyP shown in Figures 7–9 are caused by porphyrin intercalation, while the strong sites are likely due to porphyrin binding to

DNA in an outside manner, similar to the 5- and 6-coordinate compounds. The fact that the inhibition patterns due to outside binding for these porphyrins are somewhat different than those found for the 5- and 6-coordinate compounds may be due to axial ligand effects or to distortions in the polymer produced by porphyrin intercalation adjacent to a region of outside binding.

The lack of site-specific inhibition in the presence of the free base, H_2T4MPyP, may be due to the earlier observation that this compound binds to DNA with only modest or no base preference (Pasternack et al., 1983b). Should this be the case, footprinting analysis would yield no site-specific inhibition, and none was found. Attempts to observe a general decrease in enzymatic activity at all sites on the fragment as r_t was increased was complicated by porphyrin-induced DNA precipitation at high values of r_t.

Conclusions

The sequence specificities of a series of cationic metalloporphyrins, MT4MPyP, where M = Mn, Fe, Co, Ni, Cu, and Zn, has been determined with quantitative footprinting analysis. The analysis revealed that the outside-binding 5- and 6-coordinate metalloporphyrins bind in the minor groove of AT-rich regions of DNA, while the 4-coordinate structures, Ni- and CuT4MPyP, appear to bind to both AT and GC sequences of the polymer. The 5- and 6-coordinate structures produced significant site-specific increases in the cleavage rate of the enzyme, which was interpreted to be due to an increase in the available substrate DNA concentration and possibly DNA structural changes that occurred upon ligand binding. In light of the structures of the outside-binding porphyrins and their high cationic charge, binding appears to be influenced by the charged surface of DNA and/or steric effects from groups located in the minor groove of the polymer.

References

Aft, R. L., & Mueller, G. C. (1983) *J. Biol. Chem. 258*, 12069–12072.

Brenowitz, M., Senear, D. F., Shea, M. A., & Ackers, G. K. (1986) *Methods Enzymol. 130*, 132–181.

Carvlin, M. J., & Fiel, R. J. (1983) *Nucleic Acids Res. 11*, 6121–6139.

Carvlin, M. J., Datta-Grupta, N., & Fiel, R. J. (1982) *Biochem. Biophys. Res. Commun. 108*, 66–73.

Dabrowiak, J. C. (1983) *Life Sci. 32*, 2915–2931.

Dabrowiak, J. C., Skorobogaty, A., Rich, N., Vary, C. P. H., & Vournakis, J. N. (1986) *Nucleic Acids Res. 14*, 489–499.

Dickerson, R. E., & Drew, H. R. (1981) *J. Mol. Biol. 149*, 761–786.

Dougherty, G., Pilbrow, J. R., Skorobogaty, A., & Smith, T. D. (1985) *J. Chem. Soc., Faraday Trans. 1 81*, 1739–1759.

Dougherty, T. J., Lawrence, G., Kaufman, J. H., Boyle, D., Weishaupt, K. R., & Goldfarb, A. (1979) *JNCI, J. Natl. Cancer Inst. 62*, 231–238.

Drew, H. R. (1984) *J. Mol. Biol. 176*, 535–557.

Drew, H. R., & Travers, A. A. (1984) *Cell (Cambridge, Mass.) 37*, 491–502.

Fiel, R. J., Beerman, T. A., Mark, E. H., & Datta-Gupta, N. (1982) *Biochem. Biophys. Res. Commun. 107*, 1067–1074.

Fiel, R. J., Carvlin, M. J., Byrnes, R. W., & Mark, E. H. (1985) in *Molecular Basis of Cancer* (Rein, R., Ed.) Part B, pp 215–226, Liss, New York.

Galas, D. J., & Schmitz, A. (1978) *Nucleic Acids Res. 6*, 3157–3170.

Goodisman, J., & Dabrowiak, J. C. (1985) *J. Biomol. Struct. Dyn. 2*, 967–980.

Hashimota, Y., Iizima, H., & Shudo, K. (1984) *Gann 75*, 567–570.

Hoard, J. L. (1971) *Science (Washington, D.C.) 174*, 1295–1302.

Kelly, J. F., Snell, M. E., & Berenbaum, M. C. (1975) *Br. J. Cancer 31*, 237–243.

Kelly, J. M., Murphy, M. J., McConnell, D. J., & OhUigin, C. (1985) *Nucleic Acids Res. 13*, 167–184.

Kopka, M. L., Yoon, C., Goodsell, D., Pjura, P., & Dickerson, R. E. (1985a) *Proc. Natl. Acad. Sci. U.S.A. 82*, 1376–1380.

Kopka, M. L., Yoon, C., Goodsell, D., Pjura, P., & Dickerson, R. E. (1985b) *J. Mol. Biol. 183*, 553–563.

Lane, M. J., Dabrowiak, J. C., & Vournakis, J. N. (1983) *Proc. Natl. Acad. Sci. U.S.A.* 2360–3264.

Lane, M. J., Vournakis, J. N., & Dabrowiak, J. C. (1985) in *Molecular Basis of Cancer* (Rein, R., Ed.) Part B, pp 145–153, Liss, New York.

Lavery, R., & Pullman, B. (1985) *J. Biomol. Struct. Dyn. 3*, 1021–1032.

Lo, S. C., Aft, R., & Mueller, G. C. (1981) *Cancer Res. 41*, 864–870.

Lown, J. W., & Joshua, A. V. (1982) *J. Chem. Soc., Chem. Commun.*, 1298–1300.

Lown, J. W., Plenkiewicz, J., Ong, C.-W., Joshua, A. V., McGovern, J. P., & Honka, L. J. (1984) *Proceedings of the 9th International Congress on Pharmcology*, Vol. 2, pp 265–269, Macmillan, New York.

Lown, J. W., Sondhi, S. M., Ong, C.-W., Skorobogaty, A., Kishikawa, H., & Dabrowiak, J. C. (1986) *Biochemistry 25*, 5111–5117.

Maniatis, T., Fritschi, E. F., & Sambrook, J. (1982) *Molecular Cloning, A Laboratory Manual*, Cold Spring Harbor Laboratory, Cold Spring Harbor, NY.

Marzilli, L. G., Banville, D. L., Zon, G., & Wilson, W. D. (1986) *J. Am. Chem. Soc. 108*, 4188–4192.

Maxam, A., & Gilbert, W. (1980) *Methods Enzymol. 65*, 499–559.

Pasternack, R. F., Francesconi, L., Raff, D., & Spiro, E. (1973) *Inorg. Chem. 12*, 2606–2611.

Pasternack, R. F., Lee, H., Malek, P., & Spencer, C. (1977) *J. Inorg. Nucl. Chem. 39*, 1865–1870.

Pasternack, R. F., Gibbs, E. J., & Villafranca, J. J. (1983a) *Biochemistry 22*, 5409–5417.

Pasternack, R. F., Gibbs, E. J., & Villafranca, J. J. (1983b) *Biochemistry 22*, 2406–2414.

Pasternack, R. F., Autebi, A., Ehrlich, B., & Sidney, D. (1984) *J. Mol. Catal. 23*, 235–242.

Pulman, B. (1983) *J. Biomol. Struct. Dyn. 1*, 773–794.

Saenger, W. (1982) *Principles of Nucleic Acid Structure*, Springer-Verlag, New York.

Scher, W., & Friend, C. (1978) *Cancer Res. 38*, 841–849.

Schultz, P. G., & Dervan, P. B. (1984) *J. Biomol. Struct. Dyn. 1*, 1133–1147.

Van Dyke, M. W., & Dervan, P. B. (1983) *Nucleic Acids Res. 11*, 5555–5567.

Weiner, P. K., Langridge, R., Blaney, J. M., Schaefer, R., & Kollman, P. A. (1982) *Proc. Natl. Acad. Sci. U.S.A. 79*, 3754–3758.